

Photo-induced tunnel currents in Al-Al₂O₃-Au structures*

Z. Burshtein and J. Levinson

The Racah Institute of Physics, The Hebrew University of Jerusalem, Jerusalem, Israel

(Received 23 September 1974)

A study of photo-induced tunnel currents in Al-Al₂O₃-Au diode structures is presented. It includes measurements of both spectral dependence and voltage dependence. The experimental results obtained can be accounted for by an analysis based on the trapezoidal model for the oxide barrier shape. The data suggest that hot-electron attenuation in the Al₂O₃ layer is insignificant.

I. INTRODUCTION

Tunnel diodes, constructed of two metals separated by a thin (< 100 Å) insulating film, have been the subject of intensive studies, both theoretical and experimental. Much of this work has been prompted by the suggestion of Mead¹ in 1961 that such structures can serve as cold-electron emitters. It consisted of studies of current-voltage² and internal photoemission³⁻⁸ characteristics and of dark⁹⁻¹² and photo-induced¹³⁻¹⁵ emission of electrons into a vacuum. Photo-induced tunnel currents (PITC), resulting from the tunneling of photo-generated hot electrons through the insulating barrier, appeared as tails in the long-wavelength range of the internal photoemission spectra,³ and have usually been neglected. In the present work, this very range is studied in detail, both experimentally and theoretically. The type of diode chosen for investigation was Al-Al₂O₃-Au, which is relatively simple to produce and has been most extensively studied by others.²

II. EXPERIMENTAL

The tunnel diodes were produced by the following procedure. A strip of aluminum about 3000 Å thick was evaporated on a microscope slide. It was then anodically oxidized in a water solution of 3-wt. % ammonium tartrate (pH 5.5) with a constant current of about 100 μA. Various oxide thicknesses in the range 40–120 Å can be obtained by varying the voltage between the electrodes. To prevent breakdown at the edges,^{2,14} the edges were covered by two strips of Al₂O₃ about 2000 Å thick, obtained by evaporation of aluminum in an oxygen ambient at 9 × 10⁻⁴ Torr. A strip of gold was then evaporated on top (thickness 200–500 Å). The oxide thickness was determined by measuring the diode capacitance assuming a relative dielectric constant of $k = 4$.

Current-voltage characteristics of the (PITC) were obtained by illuminating the aluminum electrode with chopped light from a 2-W Spectra-Physics argon laser through the gold electrode (which is sufficiently thin to be practically transparent).

The current was measured on a series resistor with a P. A. R. HR-8 lock-in amplifier. The spectral response of the PITC could be measured only at zero voltage. The optical setup consisted of a 150-W iodine-quartz lamp and a Jarell-Ash double monochromator. The rate at which the diode electrodes were charged during illumination was measured by a Cary Model-31 vibrating-reed electrometer. The output signal was further amplified by a type-155 Keithley microvoltmeter and recorded on a Honeywell recorder. The optical transmission of the gold layer was measured by a Beckman DK spectrophotometer.

III. THEORETICAL CONSIDERATIONS

PITC will be analyzed in terms of the trapezoidal model for the barrier shape illustrated in Figs. 1(a) and 1(b), together with a number of simplifying assumptions. We restrict ourselves to excitation of hot electrons in the aluminum metal only; excitation of hot electrons in gold has been found to be much less significant.³ We further assume that in the aluminum metal all allowed energy-conserving transitions are of equal probability. As a result of optical excitation, a new energy distribution function for electrons $f^*(E)$ is established at the Al-Al₂O₃ interface. It would be a reasonable approximation to assume that the distribution function is reduced by a fraction θ in the energy range $E_F - h\nu < E < E_F$ and augmented by the same amount in the range $E_F < E < E_F + h\nu$, as illustrated in Fig. 1(c). The parameter θ is taken to be directly proportional to the light intensity F . The net current density J that tunnels from the aluminum electrode to the counter electrode is given by¹⁶

$$J = \frac{4\pi me}{h^3} \int_0^{E_{\max}} D(E_x) dE_x \int_{E_x}^{\infty} [f_1^*(E) - f_2(E)] dE. \quad (1)$$

Here $E_{\max} \equiv E_F + h\nu$ is the maximum electron energy in the aluminum electrode, E_x is the x component of the electron energy (x being the direction perpendicular to the diode surface), $D(E_x)$ is the tunneling probability for an electron having an energy component E_x , m is the effective mass of electrons

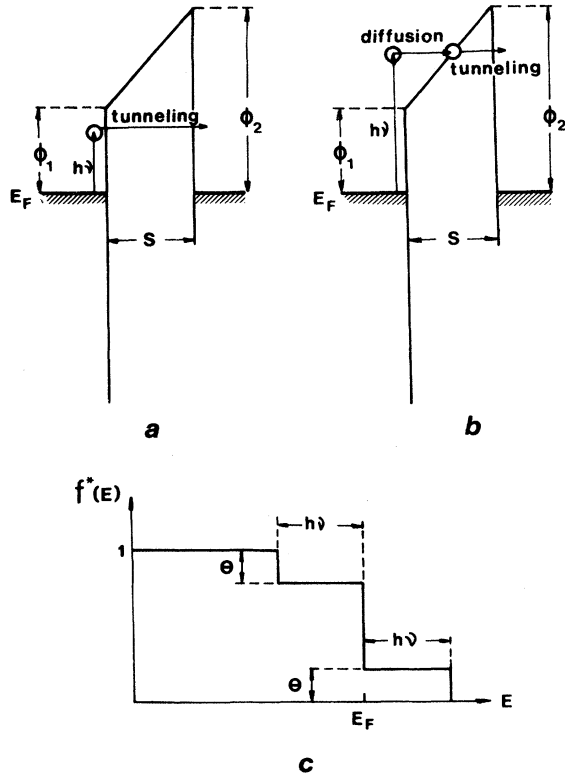


FIG. 1. Illustration of the model used for analyzing PITC: (a) $h\nu < \phi_1$; (b) $\phi_1 < h\nu < \phi_2$, the electron transport process consists, in this range, of diffusion into the conduction band of Al_2O_3 and then tunneling into the counter electrode; (c) the new distribution function of $f^*(E)$ at the Al- Al_2O_3 interface assumed to be established by illumination at photon energy $h\nu$.

in the metals, e is the electronic charge, h is Planck's constant, and $f_1^*(E)$ and $f_2(E)$ are the energy distribution functions at the aluminum and gold metal-insulator interfaces, respectively. With the above assumptions for the distribution function $f(E)$, Eq. (1) reduces to

$$J = \frac{4\pi me}{h^3} \theta \left(\int_{E_F - h\nu}^{E_F + h\nu} D(E_x) (E_F + h\nu - E_x) dE_x - 2 \int_{E_F - h\nu}^{E_F} D(E_x) (E_F - E_x) dE_x \right). \quad (2)$$

We consider three frequency ranges: long wavelengths ($h\nu < \phi_1$), intermediate wavelengths ($\phi_1 < h\nu < \phi_2$), and short wavelengths ($h\nu > \phi_2$).

A. Long-wavelength range $h\nu < \phi_1$

Following Simmons,^{17,18} we write

$$D(E_x) \approx \exp[-A(E_F + \bar{\phi} - E_x)], \quad (3)$$

where

$$A = (4\pi S/h)(2m^*)^{1/2}$$

and

$$\bar{\phi} = (1/\Delta S) \int_{S_1}^{S_2} \phi(x) dx.$$

Here, $\phi(x)$ is the potential barrier at distance x from the aluminum electrode measured from the Fermi energy, S_1 and S_2 denote the points where an electron having an energy component E_x starts and ends the tunneling process (see Fig. 1), and m^* is the electron effective mass in the oxide layer. The tunneling length $\Delta S = s_2 - s_1$ is, in this region, just the oxide thickness S .

Calculation of the first integral in (2) yields

$$\int_{E_F - h\nu}^{E_F + h\nu} \exp[-A(E_F + \bar{\phi} - E_x)^{1/2}] (E_F + h\nu - E_x) dE_x = -2 \int_{(\bar{\phi} + h\nu)}^{\bar{\phi}} e^{-Ay} [y^2 + (h\nu - \bar{\phi})] y dy, \quad (4)$$

where $y = (E_F + \bar{\phi} - E_x)^{1/2}$. After integration, one obtains

$$\frac{2}{A} e^{-Ay} \left[y^3 + \frac{3y^2}{A} + \frac{6y}{A^2} + \frac{6}{A^3} - (\bar{\phi} - h\nu) \left(\frac{1}{A} + y \right) \right] \Big|_{(\bar{\phi} + h\nu)^{1/2}}^{(\bar{\phi} - h\nu)^{1/2}}.$$

In a similar way, we obtain for the second integral

$$-\frac{4}{A} e^{-Ay} \left[y^3 + \frac{3y^2}{A} + \frac{6}{A^3} - \bar{\phi} \left(\frac{1}{A} + y \right) \right] \Big|_{(\bar{\phi} + h\nu)^{1/2}}^{\bar{\phi}^{1/2}}.$$

A typical value for A (with $S = 30\text{\AA}$) is $2.5 \times 10^7 \text{ erg}^{-1/2}$, while y varies in a range of about $(1-2) \times 10^{-6} \text{ erg}^{1/2}$. Thus, the product Ay varies in the range of about 25-50. Because of the factor e^{-Ay} , we can thus neglect the values of the functions at the limits except at the upper limit of the first integral. In this limit the term containing y^3 cancels with the last term and one has to a good approximation

$$J \approx \theta \frac{e(m/m^*)}{2\pi h S^2} (\bar{\phi} - h\nu) \times \exp\left(-\frac{4\pi S}{h} (2m^*)^{1/2} (\bar{\phi} - h\nu)^{1/2}\right), \text{ for } h\nu < \phi_1. \quad (5)$$

For the assumed trapezoidal barrier shape $\bar{\phi} = \frac{1}{2} \times (\phi_1 + \phi_2)$, one thus obtains

$$J \approx \theta \frac{e(m/m^*)}{4\pi h S^2} (\phi_1 + \phi_2 - 2h\nu) \times \exp\left(\frac{4\pi S m^*^{1/2}}{h} (\phi_1 + \phi_2 - 2h\nu)^{1/2}\right), \text{ for } h\nu < \phi_1. \quad (6)$$

This expression describes the photon-energy dependence of the PITC under zero-bias conditions. The voltage dependence of the PITC can be obtained from (6) by substituting $\phi_2 \mp eV$ for ϕ_2 , where the minus and plus signs correspond to the forward (Al electrode negative) and reverse (Al electrode positive) polarity, respectively. In the forward

polarity, this is valid only for voltages in the range $0 \leq V < (\phi_2 - h\nu)/e$.

B. Intermediate-wavelength range $\phi_1 < h\nu < \phi_2$

We assume here that electrons generated at the

$$D(E_x) = \begin{cases} \exp[-A(E_F + \frac{1}{2}\phi_1 + \frac{1}{2}\phi_2 - E_x)^{1/2}], & 0 < E_x < E_F + \phi_1 \\ \exp\left(-A \frac{(E_F + \phi_2 - E_x)^{3/2}}{\sqrt{2}\Delta\phi}\right), & E_F + \phi_1 < E_x < E_F + h\nu, \end{cases} \quad (7)$$

where $\Delta\phi = \phi_2 - \phi_1$. Substituting (7) into (2) and making similar approximations to those leading to (6), one obtains

$$J \approx \theta \frac{\Delta\phi^2 e(m/m^*)}{9\pi\hbar S^2 (\phi_2 - h\nu)} \times \exp\left(-\frac{4\pi S m^{*1/2}}{\hbar\Delta\phi} (\phi_2 - h\nu)^{3/2}\right), \quad \text{for } \phi_1 < h\nu < \phi_2. \quad (8)$$

As in the case of (6), the voltage dependence in this range will be given by substituting for ϕ_2 in (8) the expression $\phi_2 \mp eV$. The minus and plus sign correspond to the forward and reverse polarity, respectively. In the forward polarity, this is valid only for voltages in the range $0 \leq V < (\phi_2 - h\nu)/e$.

C. Short-wavelength range $h\nu > \phi_2$

If we neglect, as before, attenuation by scattering or through other energy-loss mechanisms, electrons in this range can diffuse through the oxide conduction band all the way to the gold electrode. Under these conditions it is reasonable to take for $D(E_x)$ the value of unity so that the zero-bias photocurrent can be approximated by

$$J \approx \theta \frac{4\pi m e}{\hbar^3} \int_{E_F + \phi_2}^{E_F + h\nu} (E_F + h\nu - E_x) dE_x \\ = \frac{2\pi m e}{\hbar^3} \theta (h\nu - \phi_2)^2, \quad \text{for } h\nu > \phi_2. \quad (9)$$

This is the well-known Fowler relation¹⁹ for electron photoemission. As in the cases of (6) and (8), the voltage dependence of the photocurrent is given by substituting for ϕ_2 in (9) the expression $\phi_2 \mp eV$. The minus and plus signs correspond to the forward and reverse polarity, respectively. In the forward polarity this is limited to voltages in the range $0 \leq V \leq \Delta\phi/e$. (A further reduction of the barrier is limited by ϕ_1 , the value of the barrier at the Al-Al₂O₃ interface.) In the reverse polarity, the voltages should be restricted to the range $0 \leq V < (h\nu - \phi_2)/e$.

IV. RESULTS AND DISCUSSION

Measurements of PITC were carried out on diodes of different oxide thicknesses. The oxide

surface and having an energy component E_x larger than ϕ_1 diffuse into the conduction band of the oxide without any scattering or energy loss [see Fig. 1(b)]. Such electrons have a shorter tunneling length so that

thickness was determined from capacitance measurements, assuming a relative dielectric constant $\kappa = 4$. The potential barriers ϕ_1 and ϕ_2 were determined from breaks that show up in the (dark) I - V characteristics. These breaks correspond to the voltages ϕ_1/e and ϕ_2/e (for the aluminum electrode positive and negative, respectively), above which electrons start to tunnel into the conduction band of the oxide rather than directly into the counter electrode. The values so determined are $\phi_1 = 2.0$ and $\phi_2 = 4.35$ eV, which are similar to those obtained by others, such as by Pollack and Morris² from similar I - V measurements (1.9 and 3.9 eV) and by Musatov¹³ from internal photoemission measurements (1.5 and 4.0 eV).

In principle, the results obtained could be due to hole tunneling. This possibility, however, can be immediately ruled out by the fact that the band gap of Al₂O₃ is 8.3 eV.²⁰ The average barrier for hole tunneling would then be 2.0 eV higher than that for electrons, and hole tunneling would be negligible compared to electron tunneling. This is indicated by the model in Fig. 1 by setting the valence band infinitely deep.

We consider first the spectral dependence of the PITC under zero-bias conditions. Equation (8) suggests that the logarithm of the product $\eta(\phi_2 - h\nu)$, where $\eta (= J/eF)$ is the PITC quantum yield (electrons per incident photon) should vary linearly with $(\phi_2 - h\nu)^{3/2}$. Results of PITC, obtained with a diode 45 Å thick are plotted accordingly in Fig. 2. In determining the yield η , the (measured) optical transmission of the gold layer was taken into account. The colinearity of the points in the figure shows that this dependence is indeed satisfied over more than three orders-of-magnitude variation in η . The values of $S m^{*1/2}$ and θ/F , can be estimated from the slope of the straight line in Fig. 2 and its intersection at the ordinate $(\phi_2 - h\nu = 0)$, respectively. The values so derived are $S m^{*1/2} = (2.2 \pm 0.3) \times 10^{-21} \text{ g}^{1/2} \text{ cm}$ and $\theta/F \sim 10^{-31} \text{ cm}^2 \text{ sec}$. Taking into account the uncertainty in the determination of the diode thickness S (due to the uncertainty in κ), one obtains for m^* a value of about 0.05–0.2 of the free-electron mass.

The spectral dependence of the PITC with non-

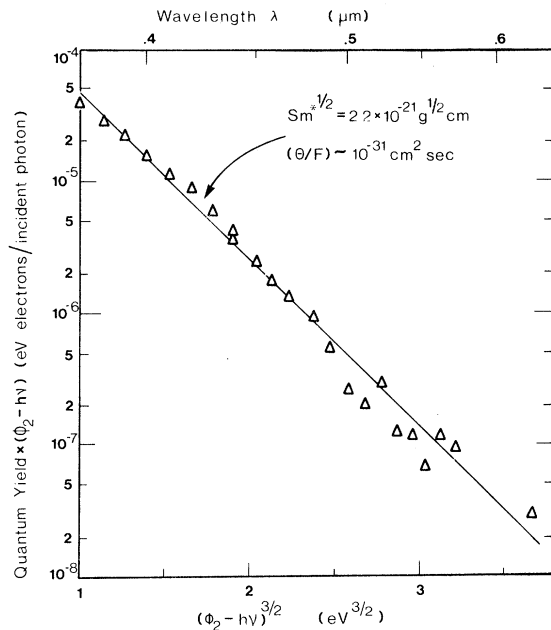


FIG. 2. Semilog plot of the product quantum yield $x(\phi_2 - h\nu)$ vs $(\phi_2 - h\nu)^{3/2}$ obtained for a diode with a 45-Å-thick layer of Al_2O_3 .

zero-bias voltage could not be measured because of the noise introduced by the dark current. However, by using a powerful laser beam with a fixed wavelength, the voltage dependence of the PITC could be measured.

In Fig. 3, the square root of the quantum yield is plotted against applied voltage for light of photon energies 2.41 and 2.71 eV (circles and triangles, respectively). The measurements were carried out with dc voltages and chopped light, they were limited to a rather narrow voltage range (1.5–3 V). At voltages below ~ 1.5 V or above ~ 3 V, the signal-to-noise ratio was poor so that the results were unreliable. Both curves show sections of linear dependence which correspond to the Fowler relation expected for voltages in the range $\Delta\phi/e > V > (\phi_2 - h\nu)/e$. The curve for $h\nu = 2.41$ eV tends to saturate for voltages above 3 V; this may indicate the onset of the regime for which $V > \Delta\phi/e$. The intersection of the Fowler plot with the abscissa yields, according to Eq. (9), the value of $(\phi_2 - h\nu)/e$. The results from Fig. 3 are 2.1 and 2.0 V for the photon energies 2.41 and 2.71 eV, respectively. Two different values, 4.5 and 4.7 eV, are thus derived for ϕ_2 , both being in reasonable agreement with the value of 4.35 eV deduced from I - V characteristics in the dark. From the slope of the Fowler plot, one derives for θ/F a value of the order of 10^{-32} $\text{cm}^2 \text{sec}$, which is in reasonable agreement with the value obtained from the spectral dependence (Fig. 2). The same order can be

derived from data reported by Shepard⁵ of internal photoemission measurements in Al- Al_2O_3 -Al structures having a similar Al_2O_3 thickness. In his case, the photon-energy dependence rather than the voltage dependence was measured.

The value expected for θ/F can be estimated from data on the optical properties of aluminum. It can be expressed by $\theta/F = \sigma\tau(1-r) = (\alpha/n)\tau(1-r)$, where σ is the cross section for photogeneration of hot electrons in aluminum, τ is the mean free time of a photoexcited electron, α is the light absorption coefficient, n is the volume concentration of electrons in aluminum, and r is the reflectivity of the Al- Al_2O_3 interface. The actual reflectivity of the aluminum layer in the diode structure under study is probably very small. This is because the light comes from the gold side, and the two metal electrodes, which have comparable reflectivities, are separated by an Al_2O_3 layer which is very thin

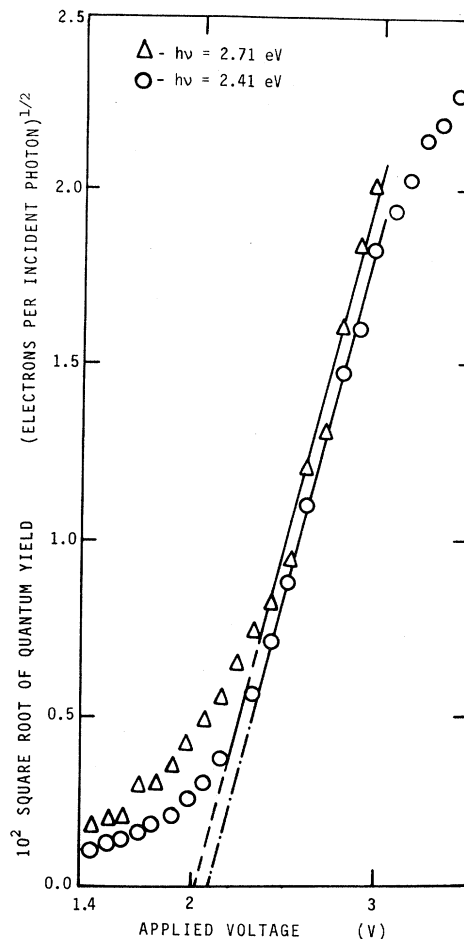


FIG. 3. Square root of quantum yield of photo-induced tunnel current as function of applied voltage (aluminum negative) at two different wavelengths. Measurements carried out with dc voltage and chopped light. Oxide thickness of 45 Å.

compared to the light wavelength. In any case, by setting $\nu=0$ in the above expression, one obtains an upper-limit estimate for θ/F . For α and n we take the values²¹ $2 \times 10^5 \text{ cm}^{-1}$ and $2 \times 10^{23} \text{ cm}^{-3}$, respectively, while τ is estimated as 10^{-14} sec . The latter estimate is based on an electron mean free path²² of 100 \AA and a Fermi velocity of 10^8 cm/sec . Using these values we obtain $\theta/F \approx 10^{-31} \text{ cm}^2 \text{ sec}$, in excellent agreement with the values obtained from the PITC data. In other words, the measured PITC are the maximum photocurrents expected.

V. CONCLUSION

A simple analysis based on the trapezoidal model for the oxide barrier shape was developed to describe photo-induced tunnel currents in metal-insulator-metal (MIM) structures. The good fit between theory and experiment indicates that the simplifying assumptions made in the analysis constitute

reasonably good approximations. The fit also justifies the neglect of electron scattering in the Al₂O₃ conduction band. This point is controversial in the literature. In some cases strong scattering in Al₂O₃ is reported,^{3,10,15} while in others^{7,8} the results suggest that hot-electron attenuation in the Al₂O₃ layer is insignificant. It appears that neither variations in the oxide thickness²³ nor the existence of an n -type transition region in the Al-Al₂O₃ interface² plays any detectable role in reducing the pre-exponential term in Eq. (8), as probably does happen² in the case of dark currents. PITC measurements thus provide an excellent tool for the investigation of MIM structures.

ACKNOWLEDGMENT

The authors are indebted to Professor A. Many for many stimulating discussions.

*Research sponsored in part by the European Research Office, U. S. Army, London, England.

¹C. A. Mead, J. Appl. Phys. **32**, 646 (1961).

²S. R. Pollack and C. E. Morris, J. Appl. Phys. **35**, 1503 (1964).

³A. Braunstein, M. Braunstein, G. S. Picus, and C. A. Mead, Phys. Rev. Lett. **14**, 219 (1965).

⁴A. I. Braunstein, M. Braunstein, and G. S. Picus, Phys. Rev. Lett. **15**, 956 (1965).

⁵K. W. Shepard, J. Appl. Phys. **36**, 796 (1965).

⁶M. Rouzeyre and B. Pistoulet, C.R. Acad. Sci. (Paris) **261**, 1653 (1965).

⁷W. Ludwig and B. Korneffel, Phys. Status Solidi **24**, K137 (1967).

⁸B. Korneffel and W. Ludwig, Phys. Status Solidi A **8**, 149 (1971).

⁹J. Cohen, J. Appl. Phys. **33**, 1999 (1962).

¹⁰H. Kanter and W. A. Feibelman, J. Appl. Phys. **33**, 3580 (1962).

¹¹R. E. Collins and L. W. Davies, Appl. Phys. Lett. **2**, 213 (1963).

¹²R. M. Handy, J. Appl. Phys. **37**, 4620 (1966).

¹³A. L. Musatov, Fiz. Tverd. Tela **9**, 3279 (1967) [Sov. Phys.-Solid State **9**, 2580 (1968)].

¹⁴P. Hartmann, G. Niquet, and P. Vernier, J. Vac. Sci. Technol. **6**, 719 (1969).

¹⁵G. Niquet, P. Vernier, and P. Hartmann, C. R. Acad. Sci. (Paris) **270**, 1234 (1970).

¹⁶See, e.g., R. C. Jaklevic and J. Lambe, in *Tunneling Phenomena in Solids*, edited by E. Burstein and S. Lundqvist (Plenum, New York, 1969), p. 245.

¹⁷J. G. Simmons, J. Appl. Phys. **34**, 1793 (1963).

¹⁸J. G. Simmons, J. Appl. Phys. **34**, 2589 (1963).

¹⁹A. L. Hughes and L. A. Dubridge, *Photoelectric Phenomena* (McGraw-Hill, New York, 1932), p. 243.

²⁰*American Institute of Physics Handbook*, 3rd. ed. (McGraw-Hill, New York, 1972), Chap. 9, p. 20.

²¹H. R. Philipp and H. Ehrenreich, J. Appl. Phys. **35**, 1416 (1964).

²²The relevant mean free path cannot be much larger than the order of the extinction depth of the light, which is about 50 \AA .

²³Z. Hurich, Solid State Electron. **13**, 683 (1969).